INFECTION AND IMMUNITY, June 2008, p. 2333–2340 Vol. 76, No. 6
0019-9567/08/$08.00+0 doi:10.1128/IAI.01515-07

Tuberculous Granulomas Are Hypoxic in Guinea Pigs, Rabbits, and Nonhuman Primates▽

Laura E. Via,[1] P. Ling Lin,[2,3] Sonja M. Ray,[1] Jose Carrillo,[1] Shannon Sedberry Allen,[4] Seok Yong Eum,[5] Kimberly Taylor,[6] Edwin Klein,[7] Ujjini Manjunatha,[1] Jacqueline Gonzales,[1] Eun Gae Lee,[1] Seung Kyu Park,[5,8] James A. Raleigh,[9] Sang Nae Cho,[10] David N. McMurray,[4] JoAnne L. Flynn,[3] and Clifton E. Barry III[1]*

Tuberculosis Research Section, Laboratory of Clinical Infectious Disease, National Institute of Allergy and Infectious Disease, National Institutes of Health, Bethesda,[1] and Comparative Medicine Branch, National Institute of Allergy and Infectious Disease, National Institutes of Health, Rockville,[6] Maryland; Department of Pediatrics, Children's Hospital of Pittsburgh,[2] and Department of Molecular Genetics and Biochemistry[3] and Division of Laboratory Animal Resources,[7] University of Pittsburgh School of Medicine, Pittsburgh, Pennsylvania; College of Medicine, Texas A&M University System Health Science Center, College Station, Texas[4]; International Tuberculosis Research Center[5] and National Masan Tuberculosis Hospital, Ministry of Health and Welfare,[8] Masan, and Department of Microbiology, Yonsei University College of Medicine, Seoul,[10] South Korea; and Department of Radiobiology, University of North Carolina School of Medicine, Chapel Hill, North Carolina[9]

Received 14 November 2007/Returned for modification 27 December 2007/Accepted 7 March 2008

Understanding the physical characteristics of the local microenvironment in which *Mycobacterium tuberculosis* resides is an important goal that may allow the targeting of metabolic processes to shorten drug regimens. Pimonidazole hydrochloride (Hypoxyprobe) is an imaging agent that is bioreductively activated only under hypoxic conditions in mammalian tissue. We employed this probe to evaluate the oxygen tension in tuberculous granulomas in four animal models of disease: mouse, guinea pig, rabbit, and nonhuman primate. Following infusion of pimonidazole into animals with established infections, lung tissues from the guinea pig, rabbit, and nonhuman primate showed discrete areas of pimonidazole adduct formation surrounding necrotic and caseous regions of pulmonary granulomas by immunohistochemical staining. This labeling could be substantially reduced by housing the animal under an atmosphere of 95% O_2. Direct measurement of tissue oxygen partial pressure by surgical insertion of a fiber optic oxygen probe into granulomas in the lungs of living infected rabbits demonstrated that even small (3-mm) pulmonary lesions were severely hypoxic (1.6 ± 0.7 mm Hg). Finally, metronidazole, which has potent bactericidal activity in vitro only under low-oxygen culture conditions, was highly effective at reducing total-lung bacterial burdens in infected rabbits. Thus, three independent lines of evidence support the hypothesis that hypoxic microenvironments are an important feature of some lesions in these animal models of tuberculosis.

Active human pulmonary tuberculosis (TB) is a chronic, complex disease in which patients present a diverse spectrum of lesions ranging from diffuse areas of inflammation and swelling of alveoli to caseous, highly organized granulomas and open cavities in intimate contact with the airways (9, 25). Computed tomography (CT) has been used to study defined types of lesions and the rate of response of such lesions to chemotherapy. Open cavities, caseous lesions, centrilobular densities (i.e., nodules or branching linear structures of 2 to 4 mm in length that are well separated from the pleural surface or the septum between pulmonary lobes), ground-glass opacities, and tissue consolidations are all apparent in active tuberculosis patients by use of this technique (17, 24, 30). The most comprehensive study of CT findings during TB chemotherapy was that of Im and colleagues (17), who studied CT scans of patients undergoing TB chemotherapy for up to 20 months and then compared their findings with postmortem autopsy results to assist in interpretation. In this study there were significant differences in the rates at which different lesion types responded to chemotherapy.

Surgical lung resection has been employed periodically as salvage therapy for patients who have failed chemotherapeutic treatment, and the resected tissues have proven useful for studying the heterogeneity of lesions that can occur within a single infected person (19, 40, 41). Studies on surgically removed tissues have revealed that most TB lesions contain surprisingly few bacilli, except for the surfaces of open cavities (19, 25, 41). Cavities are the best-oxygenated TB lesions, and most have the same oxygen tension as the communicating bronchi at apparently normal atmospheric oxygen tension (15). The bacteria within such aerobic environments are likely to be highly susceptible to conventional chemotherapies. Caseous necrotic lesions are also abundant in resected lung tissue, with thick multicellular walls insulating them from the airways of the host, and these have been reported to contain relatively fewer bacilli (21, 41). In this environment, it appears that the bacteria are less responsive to current chemotherapy (41);

* Corresponding author. Mailing address: Tuberculosis Research Section, Laboratory of Clinical Infectious Disease, National Institute of Allergy and Infectious Disease, National Institutes of Health, Bethesda, MD 20852. Phone: (301) 435-7509. Fax: (301) 480-5712. E-mail: cbarry@mail.nih.gov.

▽ Published ahead of print on 17 March 2008.

thus, increasing attention has been given to understanding the physiology of caseous, necrotic granulomas and the tubercle bacilli within them.

Within these lesions, the bacteria may exist in a state of nonreplicating persistence, during which they may have acquired a phenotypic resistance to antimycobacterial drugs (13, 26). The chemical and physical characteristics of the human microenvironments containing these nonreplicating bacilli are not known; however, since the 1950s, it has been postulated that reduced oxygen tension may be one essential feature (35–37). This concept underlies the in vitro models of hypoxia-induced nonreplicating persistence in which the growth of the organism is arrested by oxygen depletion (44). In this in vitro hypoxic state, *Mycobacterium tuberculosis* becomes phenotypically resistant to first-line antituberculosis agents such as isoniazid and ethambutol and shows reduced susceptibility to killing with rifampin (Rif) while acquiring a unique susceptibility to metronidazole (Mtz) (43, 45).

Recently, several studies have used hypoxia-imaging agents to demonstrate that mice infected with *M. tuberculosis* (which fail to produce highly organized caseous or necrotic lesions) do not develop hypoxic regions within their infected lungs (3, 39). However, in C57BL/6 mice infected with *Mycobacterium avium* strain TMC724, more-organized caseous pulmonary lesions that are positive for the hypoxia marker pimonidazole hydrochloride (PIMO) have been clearly shown (3). Guinea pigs have also been shown to produce a population of caseous lesions positive for PIMO (23). Experiments comparing C57BL/6 and gamma-interferon-deficient mice suggest that imbalanced angiostatic and angiogenic signals controlling neovascularization may contribute to caseation (2). PIMO is an investigational oncology probe used as a hypoxia-imaging agent in clinical studies to detect reduced oxygen concentrations in animal and human tumors (31–33). PIMO is able to diffuse across cell membranes and is bioreductively activated by mammalian nitroreductases at a partial pressure of oxygen (pO_2) below 10 mm Hg (14 μM) (12, 31). Upon activation, PIMO binds to thiol-containing peptides and proteins in hypoxic cells that can be detected in biopsy specimens by antibodies to the PIMO protein adduct (4, 5, 32). The oxygen concentration required for productive PIMO activation is low compared to the oxygen concentrations in venous blood and lung tissue, and the unbound agent is cleared rapidly, resulting in highly selective labeling of tissue regions that are hypoxic.

In this study, several models of TB were compared in order to try to assess the state of oxygenation of the tuberculous granuloma using the oncology probe PIMO. We found that guinea pigs, rabbits, and nonhuman primates all have lesions in the lung that stain with this probe but that murine lesions do not. The rabbit model was used to confirm that PIMO staining of TB lesions was oxygen responsive, and direct measurement of pO_2 using an oxygen-sensitive electrode showed that the oxygen tension was 2 mm Hg in these granulomas. Finally, Mtz, a drug active only against hypoxic TB, was shown to be active in rabbit infections, though it had failed to show activity in murine infections in previous investigations.

MATERIALS AND METHODS

Animals and human subjects. The studies using C57BL/6 and BALB/c mice, New Zealand White (NZW) rabbits, outbred Hartley strain guinea pigs, and adult cynomolgus macaques were performed with the approval of the animal care and use committees of NIAID, Texas A&M University, and the University of Pittsburgh. Human lung tissue collection from adult patients undergoing lung resection for the management of multidrug-resistant TB was approved by the National Masan Tuberculosis Hospital (NMTH) institutional review board and granted an exemption by the U.S. National Institutes of Health, Office of Human Subject Research. Resected lung tissue was collected for this research collaboration between NIAID and NMTH with written consent from the patients.

Bacteria and infection of animals. *Mycobacterium tuberculosis* strain HN878 (J. Musser), *M. tuberculosis* CDC1551 (Centers for Disease Control and Prevention), *M. tuberculosis* Erdman, *M. tuberculosis* H37Rv, and *Mycobacterium bovis* Ravenel and AF2122 (American Type Culture Collection) were maintained on Middlebrook 7H11 agar and frozen as described previously (34). The aerosol inocula were prepared by diluting these frozen stocks to 1×10^5 to 1.5×10^5 CFU/ml in phosphate-buffered saline (PBS)–Tween 80 (0.05%) (8). Guinea pigs were infected by low-dose aerosol as described previously with *M. tuberculosis* strain CDC1551 or H37Rv, and lungs were harvested at 4 and 8 weeks postinfection (46).

For infection of rabbits, frozen aliquots of *M. bovis* Ravenel or AF2122 or *M. tuberculosis* HN878 were inoculated into Middlebrook 7H9 medium (1:20), incubated with rolling for approximately 8 to 10 days, and adjusted to an optical density at 650 nm of 0.7. This culture was diluted 1:300 in PBS and loaded into a three-jet nebulizer (CH Technologies). Female rabbits (weight, 2.0 to 2.4 kg) were restrained in veterinary bags with hoods and loaded into the nose-only exposure tubes. This solution delivered approximately 200 CFU/liter of infectious aerosol and generated 50 to 100 granulomas per rabbit lung. Animals (n = 3) used to determine bacterial deposition were harvested 2 h postinfection.

Cynomolgus macaques (>4 years old) were infected via bronchoscopic instillation of a low dose (~25 CFU per monkey) of *M. tuberculosis* strain Erdman into the right lower lung as previously described (7). *M. tuberculosis* infection was confirmed by conversion of a negative tuberculin skin test to positive and by a lymphocyte proliferation assay in response to mycobacterial antigens. Monkeys were followed with serial clinical, radiographic, microbiologic, and immunologic assays. A total of eight monkeys were used in this study. Four of the monkeys developed active TB requiring necropsy. These represented a variety of clinical courses, including those with rapid progression after infection, worsening chronic/active disease, and spontaneous reactivation after latent infection (7). Two monkeys had clinically latent infections but were euthanized as part of other investigations. Two other monkeys had latent infections but were euthanized due to non-TB-related complications.

Treatment with PIMO, necropsy, and tissue preparation. The dose of PIMO for mice (30 to 60 mg/kg of body weight intraperitoneally [i.p.] for 2 h) was that recommended by the manufacturer. Doses that produced strong PIMO labeling of the kidney with little or no background in normal lungs were as follows: for guinea pigs, 30 mg/kg i.p. for 4 h; for rabbits, 30 mg/kg intravenously (i.v.) or i.p. for 16 to 20 h; for macaques, 20 mg/kg i.v. for 20 to 24 h. In some experiments, the oxygen content of the animal's atmosphere was altered using a ProOx controller and an A chamber (BioSpherix, Redfield, NY). Rabbits were exposed to 95% O_2 by the addition of Carbogen for 4 h prior to PIMO injections and for 16 h after administration. Control animals were housed in normal room air, and they were necropsied and their tissues processed and stained at the same times as those from altered O_2 atmospheres.

Mice were euthanized by cervical dislocation, and dissected lung and kidney tissues were preserved in 10% neutral buffered formalin for 24 h before paraffin embedding and processing. Guinea pigs were euthanized as described previously (22). Lung and kidney tissues were fixed in 10% neutral buffered formalin for a minimum of 24 h before paraffin embedding and processing. Rabbits were sedated with ketamine/xylazine, euthanized by i.v. injection of sodium pentobarbital (120 mg/kg), and immediately necropsied. The entire accessory lobe and slices of the remaining lobes were preserved in 4% paraformaldehyde in PBS (pH 7.4) (20) or 10% neutral buffered formalin for a minimum of 24 h, processed, and embedded in low-temperature paraffin wax.

At the time of necropsy, nonhuman primates were sedated (ketamine) and a lethal dose of pentobarbital was administered. Normal and granulomatous lung tissues were excised, fixed in 10% normal buffered formalin for at least 24 h, and then paraffin embedded. Resected human lung tissue was immediately dissected. Gross lesions were identified by type and subdivided for fixation as described above.

Staining and immunohistological identification of PIMO adducts. The extensive development of PIMO as an agent for imaging hypoxia within tissues has identified several tissues with regions that are normally hypoxic, including the tubules of the kidney (47). Throughout this study, we assayed the kidney of each experimental animal in the same staining run as the lung samples to confirm PIMO-positive staining of the kidney prior to scoring the lung tissue and granulomas for the presence or absence of PIMO adducts. For each tissue block, 5-μm-thick

consecutive sections were prepared, and serial sections were stained with standard hematoxylin and eosin (H&E), the Ziehl-Neelsen acid-fast procedure, and the Hypoxyprobe-1 antibody for PIMO. For detection of PIMO adducts in animal tissues, paraffin sections were deparaffinized, treated with cell conditioner 1, and incubated in succession with the Hypoxyprobe-1 antibody (1:50) for 40 min at room temperature, followed by a biotin-conjugated goat anti-mouse immunoglobulin G antibody (1:2,000; Vector Laboratories) for 32 min, the DAB (3,3-diaminobenzidine) labeling system (Ventana Medical Systems), and hematoxylin counterstaining for 4 min using a Ventana Discovery XT autoimmunostainer (Ventana Medical Systems). After staining, slides were washed with 2% Dawn (Procter and Gamble), dehydrated, and mounted with Cytoseal 60 (Richard Allen Scientific). Photographic images were captured through a Zeiss Axioskop microscope equipped with a Plan-Neofluar lens using a Retigna 1300 cooled QImaging camera and were analyzed using IPLab 3.6.1 software (Scanalytics Inc.).

Classification of granulomas into solid or caseous types. A direct terminal deoxynucleotidyltransferase-mediated dUTP-biotin nick end labeling (TUNEL) assay (*In Situ* Cell Death detection kit; Roche) was conducted on paraffin sections containing granulomas. Prior to the assay, the sections were deparaffinized and subjected to a short sodium citrate treatment using a Ventana Discovery IHC processor. The terminal transferase (TdT) and fluorescein-dUTP reaction mixture was added to the slides and incubated at 37°C to label free 3′ OH ends in genomic DNA. For each tissue, a negative control without TdT and a positive control where the section had been exposed to DNase I for 10 min prior to the TUNEL reaction were prepared and examined. The treated sections were placed on coverslips and viewed under a fluorescence microscope. Two of three independent readers scored each histology specimen in the study. During scoring, sections were coded so that animal tracking numbers and their treatments were obscured from the readers. Each reader classified granulomas by type using H&E-stained tissue sections as well as sections subjected to the TUNEL reaction. The readers scored the coded tissue sections labeled with the anti-PIMO antibody separately from the H&E-stained and TUNEL-stained sections; then a master list of animal tissue specimens, the lesions that each contained, their classification, and their staining status was constructed.

Thoracotomy procedure and oxygen measurement. NZW rabbits were infected with 300 CFU of *M. tuberculosis* strain HN878 ($n = 3$) or ~30 CFU of *M. bovis* ($n = 4$) as described above, and the infection was allowed to develop for 6 to 8 weeks prior to the thoracotomy procedure. Measurements of pO_2 were also taken for uninfected, age-matched rabbits ($n = 3$) housed in the same facility. Prior to surgery, each rabbit was administered PIMO (16 h prior) and glycopyrrolate, and each was sedated using a ketamine, xylazine, and Acepromazine mixture (20 min) prior to insertion of a 3.5-mm cuffed endotracheal tube and an angiocatheter into the lateral ear vein for i.v. saline and venous access. The tube was connected to a Bain Circuit with a rebreathing bag, and isoflurane anesthesia (1 to 1.5%) was supplied with medical air (21% oxygen). Supplemental heat was supplied by securing the animal in the left lateral recumbency on a prewarmed recirculating water blanket, and the right side was clipped and disinfected. Blood oxygen saturation, heart rate, and body temperature were measured continuously, and blood oxygen saturation remained at or above 92 during the procedures. A lidocaine line block was placed in the fifth intercostal space, and an incision was made through the skin and muscle to the pleura. The thoracic cavity was entered using blunt-tipped surgical scissors, causing the lung to collapse away from the thoracic wall. After this incision, the lungs were volume ventilated mechanically or manually 30 to 40 times/min to maintain normal oxygenation. Retractors were used to spread the ribs, and the lobes of the lung were manipulated using padded forceps.

Tissue pO_2 was measured with a four-channel fiber optic oxygen sensor (OxyLite 4000 + Oxydata; Oxford Optronix, Oxford, United Kingdom). Each probe (BF/OT/E pO_2/Temp sensor) was calibrated by the manufacturer and identified through a bar code scanned into the OxyLite sensor prior to use. The system uses a pulse of blue light (470 nm) to excite a platinum-based fluorophore embedded in a silicone matrix on the tip of the fiber and measures the duration of the resultant fluorescent signal. Since oxygen quenches the signal, the higher the dissolved O_2 concentration at the tip of the fiber, the shorter the fluorescent signal. The signal was converted as a function of temperature within the system to report absolute pO_2 in mm Hg at 1-s intervals. The data were digitized using the Oxydata system and transferred for analysis in PowerLab Chart (version 4.2.4) software (ADI Instruments, Castle Hill, Australia).

Although the probes were precalibrated, the operation of each probe was confirmed by taking pO_2 measurements of humidified, 35 to 37°C air (~151 mm Hg) and nitrogen-saturated PBS (1 to 3 mm Hg). We also measured blood pO_2 in the right atrium chamber (~40 mm Hg) and the fourth intercostal muscle (~25 mm Hg) at least once during each surgical procedure. For each rabbit, alternating measurements were taken in apparently normal lung and granulomatous lesions in the right medial and caudal lobes; for one rabbit, the right cranial lobe was also accessible to the probe. Each measurement was taken by inserting the needle-sheathed probe through the plural surface of the lung and then retracting the needle to position the probe tip ~2 mm into the targeted tissue. The probe was maintained in position for ~1 to 2 min in each location. After the measurements were made or if the animal's vital signs became unstable, the animal was euthanized using Beuthanasia-D administered via the i.v. catheter, and a full necropsy was completed.

Drug treatment of rabbits and mice, and statistical analysis. Rabbits were habituated to receive 2 ml of raspberry-flavored syrup by a 3-ml syringe daily for 3 weeks prior to drug treatment. Metronidazole benzoate (80 mg/ml) and Rifadin IV (rifampin at 20 mg/ml) were prepared and offered orally in raspberry syrup. The Rif solution was prepared and used within 15 min of mixing with syrup. Beginning 5 weeks after infection, the rabbits were treated with either 20 mg/kg Mtz twice daily, 10 mg/kg Rif once daily, or syrup alone for 4 weeks. During necropsy, the entire right midlobe was weighed and homogenized in 6 ml of M7H9 medium for CFU determination. Individual granulomas and normal tissue from the remaining lung were dissected, sized, and homogenized for CFU determination. Our experiments did not culture any *M. bovis* Ravenel in the rabbit spleen after 4 weeks.

Mice were infected with *M. bovis* Ravenel as previously described for *M. tuberculosis* (34). Beginning 5 weeks after infection, the mice were gavaged with either 20 mg/kg Mtz twice daily, 10 mg/kg Rif once daily, or PBS alone for 28 consecutive days. The doses were chosen to attempt to simulate the expected human exposure to these two agents on the basis of the fact that 10 mg/kg Rif gives a maximal concentration in serum of 10 μg/ml in mice (18), approximately the same as the maximal concentration in the sera of humans after ingestion of a single 600-mg dose (29). Interspecies allometric scaling of exposure generally correlates with the weight of the animal; thus, the exposure of rabbits should be lower than that of mice but still slightly higher than that of humans (38). After a single 500-mg dose of oral Mtz in humans, maximal concentrations in serum are approximately 5 to 10 μg/ml (16). Preliminary studies with rats indicate that after a 15-mg/kg oral dose of Mtz, maximal serum drug concentrations are also approximately 10 μg/ml (V. Dartois, unpublished data). For C57BL/6 mice given Mtz in their drinking water, serum drug concentrations were 5.9 μg/ml, suggesting comparable exposure for this species (5). During necropsy, the right lung and spleen were homogenized separately in 1 ml of M7H9 medium, diluted, and spread on M7H11 agar for CFU determination. One-way analysis of variance (ANOVA) assuming a Gaussian population distribution and Bonferroni's multiple-comparison test were used to compare the CFU data.

RESULTS

Pimonidazole labeling in *M. tuberculosis*-infected mice. *M. tuberculosis* strain H37Rv and a hypervirulent, hypoimmunogenic clinical isolate (HN878) were used to infect C57BL/6 mice ($n = 6$ for each group) and BALB/c mice ($n = 3$ for each group) by low-dose aerosol exposure (34). After a chronic infection was well established (90 to 120 days), 60 mg/kg PIMO was administered to the infected groups and to three age-matched uninfected control animals. Two hours later, the animals were sacrificed, and the extent of PIMO protein adduct formation was assessed in both the kidney tubules and lungs of infected and uninfected animals. Infected mice had numerous sites of granulomatous inflammation in their lungs but no areas of necrosis in the lung endothelium (Fig. 1A). No significant PIMO staining of lung granulomatous tissue was observed in the infected animals (Fig. 1B), nor did the normal lung sections show any significant labeling. In total, 18 chronically infected animals with 92 granulomas were examined, and no labeling of lung granulomas was observed after PIMO administration (Fig. 2B).

Pimonidazole labeling in *M. tuberculosis*-infected guinea pigs. A total of 13 guinea pigs infected with *M. tuberculosis* were dosed with PIMO 4 h before sacrifice at 4 weeks (4 animals) and 8 weeks (9 animals) postinfection. One hundred

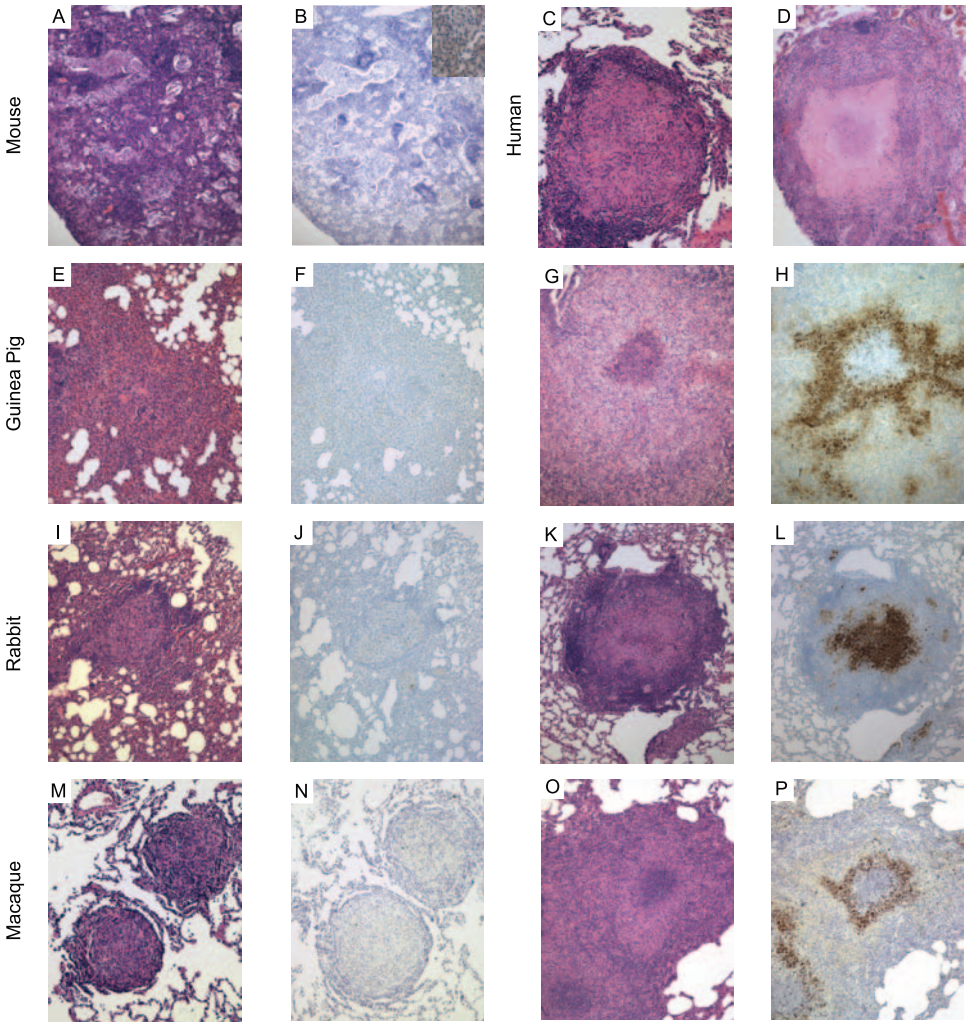

FIG. 1. Comparison of solid and caseous granulomas as revealed by H&E staining and anti-PIMO adduct labeling. Shown are granulomas from mice (A and B), humans (C and D), guinea pigs (E to H), rabbits (I to L), and macaques (M to P) infected with *M. tuberculosis* complex. Solid granulomas, lacking necrosis, are seen in human disease (C) and in each of the animal models (A, E, I, and M) and do not label strongly with PIMO (B, F, J, and N). In contrast, caseous necrotic granulomas (D, G, K, and O) have cellular regions that, in the guinea pig, rabbit, and macaque models displaying these lesions, form PIMO adducts (H, K, and P; brown coloration), indicating low oxygen tension. The murine strains lacked caseous granulomas and were not labeled with an anti-PIMO adduct antibody. The inset in panel B shows murine kidney staining with an anti-PIMO antibody from the same mouse. Resected human lung tissue was not stained with PIMO. Effective magnification, ×10.

fifty-five granulomas ranging from 0.1 to 5 mm in width were identified in right upper lobe tissue sections, and 46% of these were classified as solid, while 54% were caseous necrotic granulomas (Fig. 2A). Most solid granulomas were found to be negative for PIMO activation (Fig. 1E and F). All of the lesions classified as caseous necrotic lesions showed evidence of intense PIMO activation (Fig. 1H), and the PIMO staining colocalized with the necrotic region, often subtending an acellular region that was present in some, but not all, necrotic lesions (Fig. 1G). In contrast, only 17% of the granulomas scored as solid without apparent necrosis showed evidence of PIMO activation (Fig. 2B). These solid granulomas without observable PIMO activation were all <0.5 mm in diameter. Extensive areas of diffuse inflammatory infiltration that were uniformly PIMO negative were observed in the lungs of these animals.

Pimonidazole labeling in *M. tuberculosis*-infected rabbits. Twelve NZW rabbits were infected via aerosol with *M. bovis* Ravenel for 8 weeks before administration of PIMO, with euthanasia following 16 to 20 h later. The granulomas observed in these animals ranged from 0.5 to 8 mm in diameter. In lung sections from these rabbits, 224 total granulomas were identified and analyzed; 26% of these lesions were scored as solid and 74% as caseous necrotic (Fig. 1I to L and 2A). All caseous necrotic granulomas showed clear evidence of PIMO activation (Fig. 2B), while in contrast, only 32% of the solid granulomas were positive for PIMO activation. The immunohistochemical staining for PIMO activation in these solid granulomas, however, was less intense than that seen in necrotic granulomas (data not shown).

Pimonidazole labeling in *M. tuberculosis*-infected cynomologous macaques. Eight cynomolgus macaques, in disease states ranging from active to latent infection, were administered PIMO 20 to 24 h prior to necropsy. A total of 270 granulomas from the lungs of these animals were evaluated. Thirty-four percent of these lesions were classified as solid granulomas lacking central

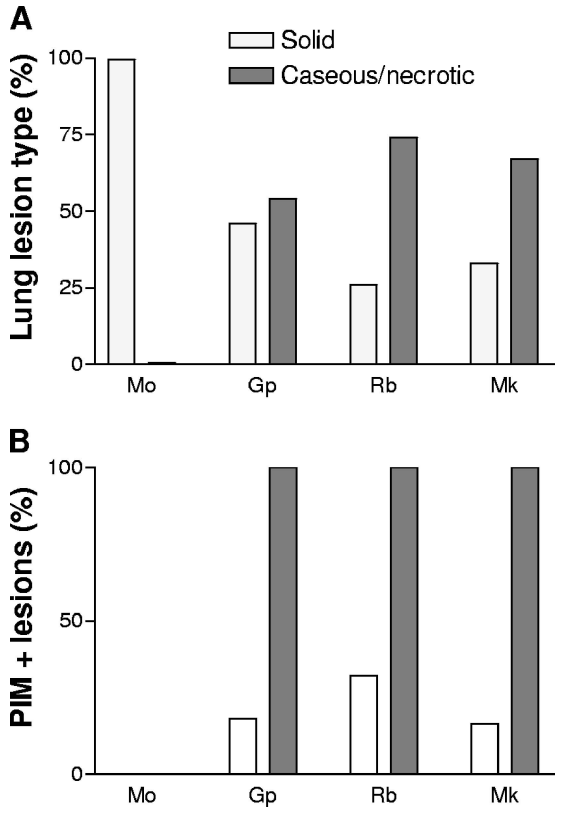

FIG. 2. Summary of pimonidazole staining by species and lesion type. (A) Summary of the distribution of granulomas, showing solid and caseous histology in each animal model. (B) Proportion of each granuloma type labeling with anti-PIMO in the animal models. Mo, mouse; Gp, guinea pig; Rb, rabbit; Mk, macaque. Open bars, solid granulomas; filled bars, caseous/necrotic granulomas.

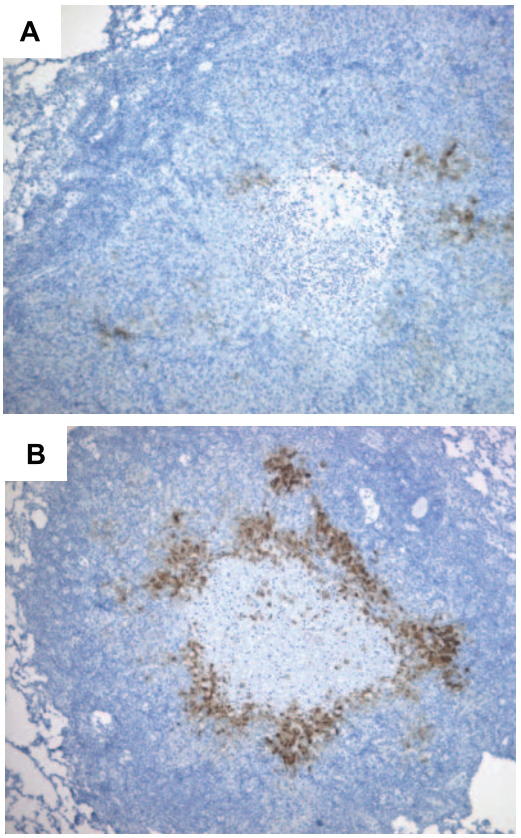

FIG. 3. Pimonidazole adduct formation is O_2 dependent in the rabbit model. (A) Necrotic granulomas showed reduced staining for activated PIMO adducts (brown coloring) after infected rabbits were housed under a 95% O_2 atmosphere during PIMO exposure. (B) Granuloma stained for activated PIMO adducts after infected rabbits were housed in normal room air. A representative granuloma is shown. Effective magnification, ×100.

caseation (Fig. 1M and 2A). Of these solid lesions, 16% demonstrated central PIMO activation (Fig. 2B). The majority of the primate lesions (66%) showed significant evidence of central caseous necrosis, and 100% of the lesions of this type showed evidence of PIMO activation, as shown in Fig. 1P. Areas of disorganized inflammatory infiltration were also observed in the lungs of three macaques, and as observed for the guinea pigs, these infiltrates did not show evidence of PIMO activation.

PIMO adduct formation in rabbits was responsive to changes in O_2 tension. To confirm that the formation of the PIMO adduct was in fact oxygen dependent in the TB model, we housed two infected NZW rabbits in an atmosphere of Carbogen (95% O_2–5% CO_2) for 4 h prior to PIMO infusion and during PIMO clearance (16 h). After exposure, rabbits were necropsied, and serial sections of the tissues were analyzed for PIMO activation by readers blinded to the treatment of the animals. PIMO staining was greatly reduced in solid and caseous granulomas of these rabbits compared to staining of similar-sized granulomas of rabbits housed in normal room air, infused with PIMO, and necropsied at the same time (Fig. 3A and B).

Direct measurement of oxygen tension in infected rabbits. We used a fiber optic probe containing both a temperature sensor and a non-O_2-consuming pO_2 sensor to measure the pO_2 directly in the lungs of live rabbits infected with either *M. bovis* or *M. tuberculosis*. NZW rabbits (uninfected or infected for 6 to 8 weeks) were anesthetized, intubated, and ventilated with medical air (21% O_2) prior to the opening of a window in the fifth intercostal space on the right side (Fig. 4A). For each rabbit, alternating measurements were taken in apparently normal lung and in granulomatous lesions if present. Each measurement was taken by inserting the needle-sheathed probe through the plural surface of the lung and then retracting the needle to position the probe tip ~2 mm into the targeted tissue. The probe was held in place for 1 min, and continuous measurements of temperature and pO_2 were recorded (Fig. 4C). Traces of data from three different granulomas and one site in the normal lung of a single animal are shown in Fig. 4C. The mean pO_2 (± standard error [SE]) for the grossly normal lungs of infected rabbits ($n = 7$) was 59.46 ± 5.03 mm Hg, not significantly different from the mean measurement for uninfected rabbits (64.15 ± 9.71 mm Hg) (Fig. 4D). Granulomas of 3 to 5 mm in *M. bovis*- and *M. tuberculosis*-infected rabbits had mean (± SE) pO_2 measurements of 2.66 ± 0.70 mm Hg and 1.61 ± 0.37 mm Hg, respectively. These oxygen partial pressures found in tuberculous lesions were significantly lower than those in the normal lung tissue ($P < 0.001$). Granulomas smaller than 3 mm could not be reliably

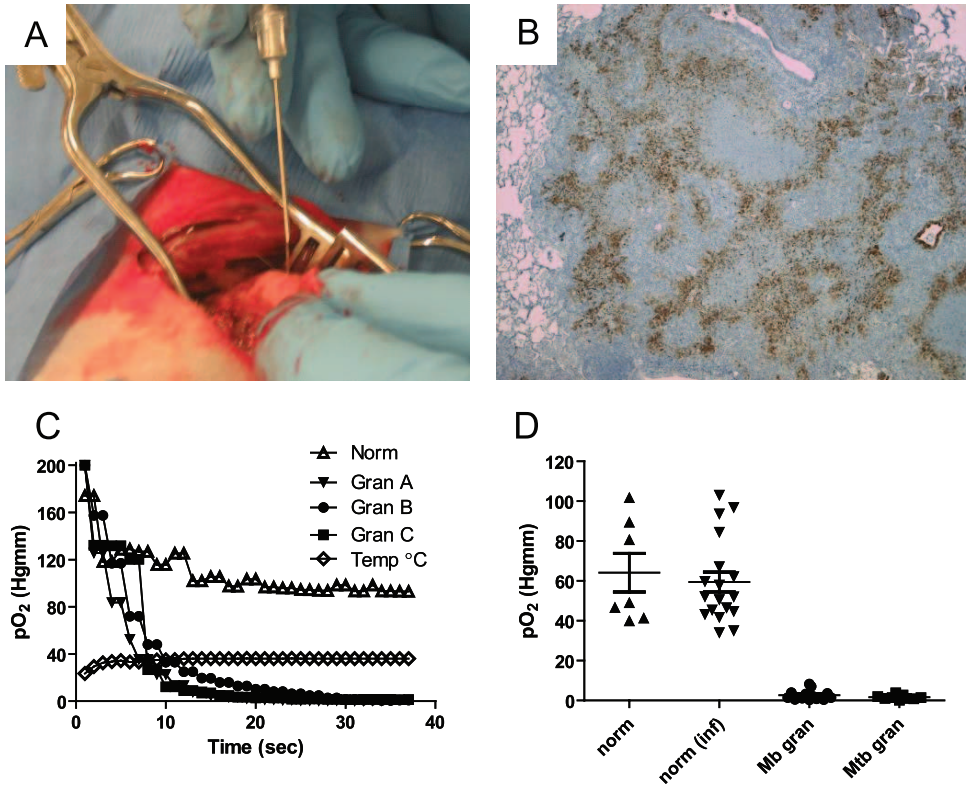

FIG. 4. Measurement of pO_2 in granulomas of *M. tuberculosis* complex-infected rabbits using a fiber optic oxygen probe. (A) After intubation and ventilation with medical air, a thoracotomy was performed and rib spreaders were used to open the thorax. The oxygen probe (sheathed in a 22-gauge needle) was inserted into visible granulomas or apparently normal portions of the lung. (B) Immunohistochemistry of an *M. tuberculosis*-induced granuloma for the hypoxia marker PIMO. Shown is a representative granuloma where pO_2 was measured (original magnification, ×50). (C) Representative traces of the response to the fiber optic pO_2-temperature probe upon insertion into normal lung or granulomas within the same rabbit. The probe was maintained in position for ~1 min in each location. (D) Summary of direct measurements of pO_2 with the fiber optic probe in lungs of uninfected rabbits (norm), grossly normal lungs in infected rabbits (norm inf), granulomas of *M. bovis*-infected rabbits (Mb gran), and granulomas of *M. tuberculosis*-infected rabbits (Mtb gran). Two to five granulomatous lesions (diameters, 3 to 5 mm) and two to three macroscopically normal areas were measured in the right medial and caudal lobes of seven infected rabbits. Two to three measurements were made in the same region for three uninfected rabbits. Each time the system was used or a probe was changed, the probe function was confirmed by measurement of pO_2 in humidified 35 to 37°C room air (~151 mm Hg) and the fourth intercostal muscle (~25 mm Hg). For each group of measurements, the horizontal line and error bar represent the mean and standard deviation. The difference in pO_2 was significant between normal lung tissue and either type of granuloma ($P < 0.001$), but there was no significant difference in pO_2 between normal-appearing lungs in uninfected or infected rabbits ($P > 0.05$) by using one way ANOVA with Tukey's posttest.

measured in the ventilated lung tissue, and the few larger granulomas observed had similar pO_2 values. Histological examination of the analyzed lesions showed caseous necrotic centers in each of the lesions measured and evidence of PIMO activation (Fig. 4B).

Efficacy of Mtz in infected rabbits. The sensitivity of *M. bovis* Ravenel to Mtz was first compared with that of *M. tuberculosis* H37Rv in the Wayne model of nonreplicating persistence. *M. bovis* Ravenel and *M. tuberculosis* had similar sensitivities to Mtz in the nonreplicating persistence 2 model (a 1.3 log reduction in CFU after 50 μM exposure for 7 days [data not shown]). Twenty-seven NZW rabbits were infected by aerogenic exposure to nebulized *M. bovis* Ravenel. Infection resulted in a mean of 101 CFU/rabbit lung (range, 76 to 141 CFU/lung) 2 h after aerogenic infection and generated an average of 53.5 granulomas (SE, ±15.5) in six untreated animals 10 weeks after infection. The remaining animals were housed for 5 weeks before being randomized into three groups ($n = 6$). Control animals received vehicle (raspberry syrup) only, Rif-treated animals received 10 mg/kg Rif in vehicle daily, and Mtz-treated animals received 20 mg/kg Mtz in vehicle twice daily. All groups were treated for 28 consecutive days.

Following 4 weeks of therapy, animals were sacrificed, and the middle lobe of each right lung was weighed, homogenized, and plated for colony enumeration, while upper and lower left lobes were dissected into individual, discrete granulomas. Several representative granulomas from each rabbit were excised, homogenized, and plated for CFU enumeration. Slices of grossly normal lung (0.5 g) were also homogenized and plated; these samples consistently had >20 CFU/g of lung. The results of one of two experiments are shown in Fig. 5. Treatment of these animals with Rif for 4 weeks resulted in a 0.73 ± 0.19 (mean ± SE) log decrease in overall CFU/g lung ($P = 0.0052$) and a 0.9 ± 0.20 log decrease in CFU/granuloma ($P = 0.0004$). Treatment with Mtz resulted in a comparable decrease in CFU/g of lung and CFU/granuloma (1.09 ± 0.0.25 [$P < 0.001$] and 1.02 ± 0.26 [$P < 0.0001$], respectively). A second experiment yielded essentially the same results.

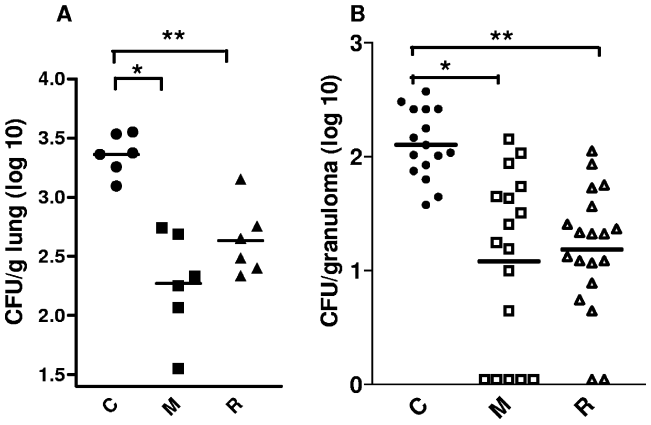

FIG. 5. Metronidazole treatment of *M. bovis* Ravenel-infected rabbits is as effective as rifampin in reducing the burden of viable bacilli. (A) Number of *M. bovis* CFU in the right middle lobe per gram of lung tissue of rabbits given 28 days of drug therapy with Mtz (M), Rif (R), or vehicle only (C) ($n = 6$ per group). A one-way ANOVA analysis returned a P value of <0.0001; the Bonferroni multiple-comparison test returned P values of <0.001 (*) for Mtz and <0.0052 (**) for Rif compared to the control. (B) Number of *M. bovis* CFU per individual 1- to 1.5-mm granuloma in the same experiment. $P < 0.0001$ by ANOVA. By the Bonferroni multiple-comparison test, $P < 0.0001$ (*) for Mtz ($n = 17$) and $P < 0.0004$ (**) for Rif ($n = 19$) compared to the control ($n = 16$).

To further confirm that this was not an *M. bovis*-specific effect, a similar treatment experiment with *M. bovis* Ravenel was conducted for C57BL/6 mice. Infected mice were housed for 5 weeks after low-dose aerosol infection before being randomized into PBS, Rif (10 mg/kg once daily), or Mtz (20 mg/kg twice daily) treatment groups. Treatment was delivered for 28 consecutive days, followed by sacrifice and lung CFU enumeration. There was no significant difference between CFU counts in lungs from control (PBS) and Mtz-treated animals, while the Rif treated animals showed a 2-log-unit reduction in CFU over the treatment period (data not shown).

DISCUSSION

While the types of inflammatory cells that constitute a granuloma appear to be the same among various animal models and in human disease, the organization and architecture differ considerably. In this study, we show that oxygen tension is reduced in necrotic, highly organized granulomas formed by guinea pigs, rabbits, and nonhuman primates, as evidenced by the formation of a stable adduct between reduced pimonidazole and host proteins. In all three animal models, both solid (cellular) and caseous (necrotic) lesions were present. The caseous granulomas uniformly stained positively for activated PIMO adducts, while the majority of solid granulomas showed little or no staining. Thus, there was nearly perfect concordance between areas of necrosis and apparent reduced oxygen tension. It is not likely that this was due to differential penetration of the drug into these similar lesions, because PIMO has been shown to penetrate even dense tumor tissue and has a high volume of distribution (1). We further show that in rabbits, the reduction in oxygen tension is profound (in the range of 2 mm of Hg) by using a fiber optic oxygen sensor inserted directly into lesions in live infected animals. This 20-fold reduction in oxygen concentration is sufficient to render the bacilli sensitive to the hypoxia-specific drug Mtz.

Murine *M. tuberculosis* lesions have recently been shown to have slightly lowered pO_2 (~37 mm Hg), but this is not sufficiently hypoxic to cause PIMO adduct formation (3) or to result in labeling with another hypoxia marker, EF5 (39). Consistent with our results, Lenearts and colleagues (23) recently demonstrated that some primary guinea pig lesions stain positively for PIMO adduct formation and hypothesized that the hypoxic lesions may be a site of persistent infection.

The presence of hypoxic microenvironments within some granulomatous lesions has the potential to alter the metabolism of *M. tuberculosis* through induction of the oxygen-sensitive *dosR* transcriptional regulon and therefore to alter susceptibility to certain antituberculosis agents (42). In fact, one of the defining characteristics of anaerobically adapted *M. tuberculosis* in vitro is sensitivity to Mtz (45), a drug with potent anti-anaerobe activity that has been evaluated in mouse models by several authors. In one murine study using the Cornell model of latent disease, addition of Mtz to either the sterilization phase or the "latent" phase of the model did not reduce the likelihood of relapse (11). In a second study, Mtz had no utility either as monotherapy or in combination with isoniazid during early active infection; however, Mtz treatment during chronic infection produced a small but significant reduction in the pulmonary bacillary load (6). In a third study, Mtz combined with isoniazid or Rif late in the course of treatment resulted in a slight reduction in bacillary loads in lung and spleen (28). In aggregate, then, the data for mice are consistent with a largely normoxic environment in murine granulomas. The results showing lack of activity in mice are unlikely to be due to poor pharmacokinetics of the drug, since previous studies have demonstrated comparable exposure for this strain of mice (5). Our data in the rabbit model demonstrate that Mtz had antimycobacterial efficacy as potent as that of Rif, the cornerstone of modern TB chemotherapy. One small study of Mtz with humans did report clinical benefit in the radiographic resolution of TB in patients but focused primarily on the rate of sputum conversion and concluded that this agent had little utility (10). Sputum-borne organisms would not be expected to be affected by Mtz, because they are most likely to have been exposed to oxygen while at the well-oxygenated surfaces of pulmonary lesions. It remains to be seen whether Mtz will have a significant benefit for human TB patients, but clinical trials to explore this possibility are under way (http://clinicaltrials.gov, ID number NCT00425113).

These studies demonstrate that valuable information can be obtained from animal models of tuberculous chemotherapy that develop hypoxic lesions and highly structured, necrotic granulomas (14, 27). Hypoxia is, of course, only one physical characteristic of necrotic lesions that distinguishes them from cavities and other granulomas. Additional work to define all of the important parameters affecting bacillary metabolism in the full spectrum of lesions found will allow a rational approach to identifying vulnerable elements in nonreplicating bacteria and enable the development of strategies to rapidly eradicate these recalcitrant populations.

ACKNOWLEDGMENTS

This research was supported by the Intramural Research Program of the NIH, NIAID (to C.E.B.), a grant from the Bill and Melinda Gates Foundation and the Wellcome Trust through the Grand Challenges in Global Health Initiative (to C.E.B., J.L.F., and S.N.C.), the National Institutes of Health (RO1 AI37895 and HL75845 to J.L.F., KO8 AI63101 to P.L.L., and R01 AI15495 to D.N.M.), and the Ellison Medical Foundation (to J.L.F.).

REFERENCES

1. **Allen, J. G., S. Dische, I. Lenox-Smith, S. L. Malcolm, and M. I. Saunders.** 1984. The pharmacokinetics of a new radiosensitiser, Ro 03-8799 in humans. Eur. J. Clin. Pharmacol. **27:**483–489.
2. **Aly, S., T. Laskay, J. Mages, A. Malzan, R. Lang, and S. Ehlers.** 2007. Interferon-gamma-dependent mechanisms of mycobacteria-induced pulmonary immunopathology: the role of angiostasis and CXCR3-targeted chemokines for granuloma necrosis. J. Pathol. **212:**295–305.
3. **Aly, S., K. Wagner, C. Keller, S. Malm, A. Malzan, S. Brandau, F. C. Bange, and S. Ehlers.** 2006. Oxygen status of lung granulomas in *Mycobacterium tuberculosis*-infected mice. J. Pathol. **210:**298–305.
4. **Arteel, G. E., R. G. Thurman, and J. A. Raleigh.** 1998. Reductive metabolism of the hypoxia marker pimonidazole is regulated by oxygen tension independent of the pyridine nucleotide redox state. Eur. J. Biochem. **253:**743–750.
5. **Arteel, G. E., R. G. Thurman, J. M. Yates, and J. A. Raleigh.** 1995. Evidence that hypoxia markers detect oxygen gradients in liver: pimonidazole and retrograde perfusion of rat liver. Br. J. Cancer **72:**889–895.
6. **Brooks, J. V., S. K. Furney, and I. M. Orme.** 1999. Metronidazole therapy in mice infected with tuberculosis. Antimicrob. Agents Chemother. **43:**1285–1288.
7. **Capuano, S. V., III, D. A. Croix, S. Pawar, A. Zinovik, A. Myers, P. L. Lin, S. Bissel, C. Fuhrman, E. Klein, and J. L. Flynn.** 2003. Experimental *Mycobacterium tuberculosis* infection of cynomolgus macaques closely resembles the various manifestations of human *M. tuberculosis* infection. Infect. Immun. **71:**5831–5844.
8. **Dahl, J. L., C. N. Kraus, H. I. Boshoff, B. Doan, K. Foley, D. Avarbock, G. Kaplan, V. Mizrahi, H. Rubin, and C. E. Barry III.** 2003. The role of RelMtb-mediated adaptation to stationary phase in long-term persistence of *Mycobacterium tuberculosis* in mice. Proc. Natl. Acad. Sci. USA **100:**10026–10031.
9. **Dannenberg, A. M.** 2006. Pathogenesis of human pulmonary tuberculosis: insights from the rabbit model. ASM Press, Washington, DC.
10. **Desai, C. R., S. Heera, A. Patel, A. B. Babrekar, A. A. Mahashur, and S. R. Kamat.** 1989. Role of metronidazole in improving response and specific drug sensitivity in advanced pulmonary tuberculosis. J. Assoc. Physicians India **37:**694–697.
11. **Dhillon, J., B. W. Allen, Y. M. Hu, A. R. Coates, and D. A. Mitchison.** 1998. Metronidazole has no antibacterial effect in Cornell model murine tuberculosis. Int. J. Tuberc. Lung Dis. **2:**736–742.
12. **Durand, R. E., and J. A. Raleigh.** 1998. Identification of nonproliferating but viable hypoxic tumor cells in vivo. Cancer Res. **58:**3547–3550.
13. **Gomez, J. E., and J. D. McKinney.** 2004. *M. tuberculosis* persistence, latency, and drug tolerance. Tuberculosis (Edinburgh) **84:**29–44.
14. **Grosset, J., N. Lounis, C. Truffot-Pernot, R. J. O'Brien, M. C. Raviglione, and B. Ji.** 1998. Once-weekly rifapentine-containing regimens for treatment of tuberculosis in mice. Am. J. Respir. Crit. Care Med. **157:**1436–1440.
15. **Haapanen, J. H., I. Kass, G. Gensini, and G. Middlebrook.** 1959. Studies on the gaseous content of tuberculous cavities. Am. Rev. Respir. Dis. **80:**1–5.
16. **Idkaidek, N. M., and N. M. Najib.** 2000. Enhancement of oral absorption of metronidazole suspension in humans. Eur. J. Pharm. Biopharm. **50:**213–216.
17. **Im, J. G., H. Itoh, Y. S. Shim, J. H. Lee, J. Ahn, M. C. Han, and S. Noma.** 1993. Pulmonary tuberculosis: CT findings—early active disease and sequential change with antituberculous therapy. Radiology **186:**653–660.
18. **Jayaram, R., S. Gaonkar, P. Kaur, B. L. Suresh, B. N. Mahesh, R. Jayashree, V. Nandi, S. Bharat, R. K. Shandil, E. Kantharaj, and V. Balasubramanian.** 2003. Pharmacokinetics-pharmacodynamics of rifampin in an aerosol infection model of tuberculosis. Antimicrob. Agents Chemother. **47:**2118–2124.
19. **Kaplan, G., F. A. Post, A. L. Moreira, H. Wainwright, B. N. Kreiswirth, M. Tanverdi, B. Mathema, S. V. Ramaswamy, G. Walther, L. M. Steyn, C. E. Barry III, and L. G. Bekker.** 2003. *Mycobacterium tuberculosis* growth at the cavity surface: a microenvironment with failed immunity. Infect. Immun. **71:**7099–7108.
20. **Kaplan, G., W. C. Van Voorhis, E. N. Sarno, N. Nogueira, and Z. A. Cohn.** 1983. The cutaneous infiltrates of leprosy. A transmission electron microscopy study. J. Exp. Med. **158:**1145–1159.
21. **Kennedy, H. E., H. M. Vandiviere, I. G. Melvin, and H. S. Willis.** 1957. The treated pulmonary lesion and its tubercle bacillus. III. Drug susceptibility studies. Am. J. Med. Sci. **233:**676–684.
22. **Lasco, T. M., O. C. Turner, L. Cassone, I. Sugawara, H. Yamada, D. N. McMurray, and I. M. Orme.** 2004. Rapid accumulation of eosinophils in lung lesions in guinea pigs infected with *Mycobacterium tuberculosis*. Infect. Immun. **72:**1147–1149.
23. **Lenaerts, A. J., D. Hoff, S. Aly, S. Ehlers, K. Andries, L. Cantarero, I. M. Orme, and R. J. Basaraba.** 2007. Location of persisting mycobacteria in a guinea pig model of tuberculosis revealed by r207910. Antimicrob. Agents Chemother. **51:**3338–3345.
24. **Long, R., B. Maycher, A. Dhar, J. Manfreda, E. Hershfield, and N. Anthonisen.** 1998. Pulmonary tuberculosis treated with directly observed therapy: serial changes in lung structure and function. Chest **113:**933–943.
25. **Loring, W. E., and H. M. Vandiviere.** 1956. The treated pulmonary lesion and its tubercle bacillus. I. Pathology and pathogenesis. Am. J. Med. Sci. **232:**20–29.
26. **McKinney, J. D., and J. E. Gomez.** 2003. Life on the inside for *Mycobacterium tuberculosis*. Nat. Med. **9:**1356–1357.
27. **Nuermberger, E. L., T. Yoshimatsu, S. Tyagi, K. Williams, I. Rosenthal, R. J. O'Brien, A. A. Vernon, R. E. Chaisson, W. R. Bishai, and J. H. Grosset.** 2004. Moxifloxacin-containing regimens of reduced duration produce a stable cure in murine tuberculosis. Am. J. Respir. Crit. Care Med. **170:**1131–1134.
28. **Paramasivan, C. N., G. Kubendiran, and D. Herbert.** 1998. Action of metronidazole in combination with isoniazid and rifampicin on persisting organisms in experimental murine tuberculosis. Indian J. Med. Res. **108:**115–119.
29. **Peloquin, C. A., R. Namdar, M. D. Singleton, and D. E. Nix.** 1999. Pharmacokinetics of rifampin under fasting conditions, with food, and with antacids. Chest **115:**12–18.
30. **Poey, C., F. Verhaegen, J. Giron, J. Lavayssiere, P. Fajadet, and B. Duparc.** 1997. High resolution chest CT in tuberculosis: evolutive patterns and signs of activity. J. Comput. Assist. Tomogr. **21:**601–607.
31. **Raleigh, J. A., D. P. Calkins-Adams, L. H. Rinker, C. A. Ballenger, M. C. Weissler, W. C. Fowler, Jr., D. B. Novotny, and M. A. Varia.** 1998. Hypoxia and vascular endothelial growth factor expression in human squamous cell carcinomas using pimonidazole as a hypoxia marker. Cancer Res. **58:**3765–3768.
32. **Raleigh, J. A., S. C. Chou, E. L. Bono, D. E. Thrall, and M. A. Varia.** 2001. Semiquantitative immunohistochemical analysis for hypoxia in human tumors. Int. J. Radiat. Oncol. Biol. Phys. **49:**569–574.
33. **Raleigh, J. A., S. C. Chou, D. P. Calkins-Adams, C. A. Ballenger, D. B. Novotny, and M. A. Varia.** 2000. A clinical study of hypoxia and metallothionein protein expression in squamous cell carcinomas. Clin. Cancer Res. **6:**855–862.
34. **Reed, M. B., P. Domenech, C. Manca, H. Su, A. K. Barczak, B. N. Kreiswirth, G. Kaplan, and C. E. Barry III.** 2004. A glycolipid of hypervirulent tuberculosis strains that inhibits the innate immune response. Nature **431:**84–87.
35. **Sever, J. L., and G. P. Youmans.** 1957. The enumeration of nonpathogenic viable tubercle bacilli from the organs of mice. Am. Rev. Tuberc. **75:**280–294.
36. **Sever, J. L., and G. P. Youmans.** 1957. Enumeration of viable tubercle bacilli from the organs of nonimmunized and immunized mice. Am. Rev. Tuberc. **76:**616–635.
37. **Sever, J. L., and G. P. Youmans.** 1957. The relation of oxygen tension to virulence of tubercle bacilli and to acquired resistance in tuberculosis. J. Infect. Dis. **101:**193–202.
38. **Shim, H. J., Y. C. Kim, J. H. Lee, J. W. Kwon, W. B. Kim, Y. G. Kim, S. H. Kim, and M. G. Lee.** 2005. Interspecies pharmacokinetic scaling of DA-8159, a new erectogenic, in mice, rats, rabbits and dogs, and prediction of human pharmacokinetics. Biopharm. Drug Dispos. **26:**269–277.
39. **Tsai, M. C., S. Chakravarty, G. Zhu, J. Xu, K. Tanaka, C. Koch, J. Tufariello, J. Flynn, and J. Chan.** 2006. Characterization of the tuberculous granuloma in murine and human lungs: cellular composition and relative tissue oxygen tension. Cell. Microbiol. **8:**218–232.
40. **Ulrichs, T., G. A. Kosmiadi, S. Jorg, L. Pradl, M. Titukhina, V. Mishenko, N. Gushina, and S. H. Kaufmann.** 2005. Differential organization of the local immune response in patients with active cavitary tuberculosis or with nonprogressive tuberculoma. J. Infect. Dis. **192:**89–97.
41. **Vandiviere, H. M., W. E. Loring, I. Melvin, and S. Willis.** 1956. The treated pulmonary lesion and its tubercle bacillus. II. The death and resurrection. Am. J. Med. Sci. **232:**30–37.
42. **Voskuil, M. I., K. C. Visconti, and G. K. Schoolnik.** 2004. *Mycobacterium tuberculosis* gene expression during adaptation to stationary phase and low-oxygen dormancy. Tuberculosis (Edinburgh) **84:**218–227.
43. **Wayne, L. G., and L. G. Hayes.** 1996. An in vitro model for sequential study of shiftdown of *Mycobacterium tuberculosis* through two stages of nonreplicating persistence. Infect. Immun. **64:**2062–2069.
44. **Wayne, L. G., and C. D. Sohaskey.** 2001. Nonreplicating persistence of *Mycobacterium tuberculosis*. Annu. Rev. Microbiol. **55:**139–163.
45. **Wayne, L. G., and H. A. Sramek.** 1994. Metronidazole is bactericidal to dormant cells of *Mycobacterium tuberculosis*. Antimicrob. Agents Chemother. **38:**2054–2058.
46. **Wiegeshaus, E. H., D. N. McMurray, A. A. Grover, G. E. Harding, and D. W. Smith.** 1970. Host-parasite relationships in experimental airborne tuberculosis. 3. Relevance of microbial enumeration to acquired resistance in guinea pigs. Am. Rev. Respir. Dis. **102:**422–429.
47. **Zhong, Z., G. E. Arteel, H. D. Connor, M. Yin, M. V. Frankenberg, R. F. Stachlewitz, J. A. Raleigh, R. P. Mason, and R. G. Thurman.** 1998. Cyclosporin A increases hypoxia and free radical production in rat kidneys: prevention by dietary glycine. Am. J. Physiol. **275:**F595–F604.

Editor: F. C. Fang